C. R. Palevol 16 (2017) 425–439

Contents lists available at ScienceDirect

Comptes Rendus Palevol

www.sciencedirect.com

General Palaeontology, Systematics and Evolution (Evolutionary Processes)

Dorsal rib histology of dinosaurs and a crocodylomorph from western Portugal: Skeletochronological implications on age determination and life history traits

Histologie des côtes dorsales de dinosaures et d'un crocodile de l'Ouest du Portugal : implications squelettochronologiques sur la détermination de l'âge et des traits d'histoire de vie

Katja Waskow [a,*], Octavio Mateus [b,c]

[a] *Steinmann Institute for Geology, Mineralogy, and Paleontology, University of Bonn, Nussallee 8, 53113 Bonn, Germany*
[b] *Departamento de Ciências da Terra, Faculdade de Ciências e Tecnologia, FCT, Universidade Nova de Lisboa, 2829-526 Caparica, Portugal*
[c] *Museu Da Lourinhã, Rua João Luis de Moura, 2530-157 Lourinhã, Portugal*

ARTICLE INFO

Article history:
Received 1st December 2014
Accepted after revision 20 January 2017
Available online 19 April 2017

Handled by Michel Laurin

Keywords:
New histological approach for ribs
Determination of ontogenetic stage
Skeletal maturity
Age at first reproduction
Longevity in dinosaurs

ABSTRACT

Bone histology is an important tool for uncovering life history traits of extinct animals, particularly those that lack modern analogs, such as the non-avian dinosaurs. In most studies, histological analyses preferentially focus on long bones for understanding growth rates and determining age. Here we show, by analyzing ornithischians (a stegosaur and an ornithopod), saurischians (a sauropod and a theropod), and a crocodile, rib histology is a suitable alternative. The estimated age for all sampled taxa ranges between 14 to 17 years for *Lourinhanosaurus antunesi* and 27 to 31 years estimated for *Draconyx loureiroi*. The theropod *Baryonyx* was skeletally mature around 23–25 years of age but showed unfused neurocentral sutures, a paedomorphic feature possibly related to aquatic locomotion. Our results show that ribs can contain a nearly complete growth record, and reveal important information about individual age, point of sexual maturity, and, in some cases, sex. Because ribs are more available than long bones, this method opens new possibilities for studying rare and incomplete fossils, including holotypes.

Mots clés :
Nouvelle approche histologique pour les côtes
Détermination du stade ontogénétique
Maturité squelettique
Âge à la première reproduction
Longévité chez les dinosaures

RÉSUMÉ

L'histologie osseuse révèle d'importantes informations sur les traits d'histoire de vie des animaux éteints n'ayant pas d'analogues modernes, comme les dinosaures non aviens. En général, les os longs sont préférés pour les analyses histologiques. En collectant des données histologiques sur les côtes de différents taxons de vertébrés fossiles tels que des ornithischiens (un stégosaure et un ornithopode), des saurischiens (un sauropode et un théropode) et un crocodile, nous montrons que l'histologie des côtes est un outil approprié pour l'étude des traits d'histoire de vie. Nos résultats montrent que les côtes renferment un enregistrement de la croissance presque complet et, avec cela, d'importantes informations

* Corresponding author.
E-mail addresses: waskow@uni-bonn.de (K. Waskow), omateus@fct.unl.pt (O. Mateus).
URL: http://docentes.fct.unl.pt/omateus (O. Mateus).

http://dx.doi.org/10.1016/j.crpv.2017.01.003
1631-0683/

sur l'âge individuel, l'âge de maturité sexuelle et parfois le sexe de l'animal. L'âge estimé de tous les spécimens échantillonnés varie entre 14 et 17 ans (*Lourinhanosaurus antunesi* ; subadultes) et 27 et 31 ans (*Draconyx loureiroi* ; adultes). Le théropode *Baryonyx* a atteint sa maturité squelettique vers 23–25 ans, mais montre des sutures du neurocentre non fusionnées, une stratégie pédomorphique qui pourrait être liée à la locomotion aquatique. Les côtes étant plus accessibles que les os longs, cette méthode ouvre de nouvelles perspectives pour l'étude de spécimens rares et incomplets, ou même d'holotypes.

1. Introduction

Non-avian dinosaurs are the best-known extinct taxa. Unfortunately, these large creatures lack modern analogs, making it difficult to reconstruct their age and growth. Osteological features like neurocentral fusion are often used to estimate the ontogenetic age of archosaurs. However, even if the closure of neurocentral sutures in pseudosuchians seems to be a plesiomorphic feature (Brochu, 1996; Ikejiri, 2012), the reliability of this diagnosis in other archosaurs is still controversial (Fronimos and Wilson, 2017; Irmis, 2007). Therefore, to obtain information about their life history, the growth record preserved in hard tissues can be used (Castanet, 1994; Castanet et al., 1993). Within the fields of bone histology and skeletochronology, important data can be obtained concerning growth rates, individual age, longevity, skeletal-, and, in some cases, sexual maturity (e.g., Curry, 1999; Enlow and Brown, 1956, 1957, 1958; Griebeler et al., 2013; Horner et al., 1999; Klein and Sander, 2007, 2008; Klein et al., 2009; de Ricqlès, 1975, 1976; de Ricqlès et al., 2001; Sander, 2000; Sander et al., 2011; Woodward et al., 2011a, 2011b). The majority of paleo-histological studies focus on the long bone diaphysis (caused by their nearly circumferential shape, making it possible to infer growth curves). A few former studies, however, have used rib histology of extinct vertebrates (e.g., D'Emic et al., 2015; Erickson et al., 2004; Houssaye and Bardet, 2012; Waskow and Sander, 2014). In contrast to extant reptiles and other non-avian dinosaurs, sauropod long bone histology lacks a skeletochronological significant growth record; thus, rib histology is needed to obtain information about their age, growth, and life cycles. In their histological study on the ribcage of the nearly complete and articulated *Camarasaurus* sp. (SMA 0002), Waskow and Sander (2014) determined that the proximal end of a rib shaft contains the most complete growth record within sauropods. Fossil ribs are generally more frequently preserved and not as important for exhibitions as long bones; thus, they are more easily accessible for analyses. The current study focuses on rib histology of different Portuguese vertebrate taxa (mainly non-avian dinosaurs) to determine whether ribs provide sufficient histological data on life history traits of dinosaurs and other vertebrates.

1.1. Growth record preservation in primary bone tissue

Growth in bone tissue is recorded by the formation of annuli. Each annulus represents the bone tissue that was deposited during one year. The most important features concerning annularity used in this study are lines of arrested growth (LAGs), which are clearly developed thin, continuous, dark lines completing the single annuli. These LAGs represent the former surface of the bone where growth was interrupted. Another form of growth lines are polish lines. These more diffuse structures are not observable under the microscope, but they are only visible by tilting a polished bone surface, in order to reflect light. They are easy to see with the naked eye (Sander, 2000). Interpretations of the annual nature of the cyclicity preserved in primary bone tissues of several skeletal elements, like the humerus and femur, have been controversial in the past (e.g., Chinsamy and Hillenius, 2004; Padian and Horner, 2004). Nevertheless, annularity of growth cycles has been demonstrated in long bones, as well as other skeletal elements such as the scapula, coracoid, and ribs of extant and extinct reptiles such as *Alligator mississippiensis* or varanid squamates (e.g., Erickson et al., 2003; Garcia, 2011; Smirina and Ananjeva, 2007; Smirina and Tsellarius, 1996; Woodward et al., 2014) and extant mammals (e.g., several ruminants) with very similar histology to that of non-avian dinosaurs (Köhler et al., 2012). Furthermore, counting lines of arrested growth (LAGs) is a standard method of aging both ectothermic (actinopterygians, lissamphibians, squamates and crocodillomorphs) and endothermic (mammals) vertebrates (e.g., Altunişik et al., 2014; Caetano, 1990; Castanet and Smirina, 1990; Castanet et al., 1993, 2004; Hutton, 1986; Pancharatna and Kumbar, 2013; Snover et al., 2013). Therefore, the annual cyclicity of growth marks is generally accepted for non-avian dinosaurs (Erickson, 2005; Sander et al., 2011). Also, it is well-established that the presence of an External Fundamental System (EFS) indicates skeletal maturity (Chinsamy-Turan, 2005; Erickson, 2005; Sander, 2000; Sander et al., 2011; Turvey et al., 2005). The annularity of LAGs within the EFS is, however, controversial. The close spacing of the LAGs with no significant histological elements like osteons or vascular canals in between can be interpreted in different ways: either as a shorter timeframe (more than one LAG deposited in a year) or a longer timeframe (LAGs deposited only every second or third year) (Horner et al., 1999). Additionally, some LAGs might be more distinct than others, and some might be partly erased by the remodeling process.

In some cases, cyclicity only appears as a polish line, which is defined as a growth line in fibrolamellar bone that is visible in a polished section but not in a thin section (Sander, 2000), or as a modulation of bone tissue

not completed by a LAG (de Ricqlès, 1983; Sander et al., 2004).

1.2. Rib histology in non-avian dinosaurs and other vertebrates

In contrast to long bones, ribs have not been a focus of scientific study for decades. Nopcsa (1933), in an innovative study for that time, was the first to analyze dinosaur rib histology using ornithopod ribs. Only a few recent histological papers focused on ribs (e.g., de Buffrénil et al., 1990; D'Emic et al., 2015; Waskow and Sander, 2014). Canoville et al. (2016) published the first quantitative exploratory study about the microanatomical diversity of amniote ribs. A few histological studies compared the dorsal rib histology of some dinosaurs with other skeletal elements (Erickson, 2005; Erickson et al., 2004; de Ricqlès et al., 2008). Most papers that take rib histology into account concern marine vertebrates (e.g., Hayashi et al., 2013; Houssaye, 2009, 2013; Houssaye and Bardet, 2012; Laurin et al., 2007). More recently, Klein et al. (2012) stated that sauropod neck ribs are ossified tendons. The first study focusing exclusively on sauropod rib histology was done by Waskow and Sander (2014). The lack of focus on ribs is primarily because humeri and femora, for example, allow growth curve calculations based on skeletochronology (caused by their nearly circumferential shape).

1.3. Differences in growth records between long bones and ribs

The study of Waskow and Sander (2014) shows that, in contrast to long bones that have most of the growth record preserved in the midshaft region (Currey, 2002; Hall, 2005), ribs, due to their growth trajectory from proximal to distal end, have the most complete growth record at the proximal end of the rib shaft. According to Amprino's rule (Amprino, 1947), the primary bone structure is closely related to the bone apposition rate. This rule has been tested and confirmed in several studies related to vertebrate long bones (Castanet et al., 1996; de Margerie et al., 2004; de Ricqlès et al., 1991), but in ribs, the relative bone apposition rate is also related to morphological changes during ontogeny, as determined by the histological rib section series of Waskow and Sander (2014). In addition, ribs grow much more slowly than long bones, which causes a difference in bone tissue type, remodeling rate, or number of preserved LAGs, even within the same individual (Horner et al., 2000; Waskow and Sander, 2014; Woodward et al., 2014). The differences in the LAG number counted in different skeletal elements of a same individual can also be explained by different resorption rates during the expansion of the medullary cavity and the difference in the degree and rate of remodeling (Waskow and Sander, 2014). The fast-growing fibrolamellar bone is also more strongly influenced by Haversian remodeling than the slower-growing lamellar-zonal bone (Chinsamy-Turan, 2005; Enlow and Brown, 1956). Moreover, the mechanical forces and loads that affect a bone differ in the individual skeletal parts and might therefore influence the primary bone tissue type (Currey, 2002; Dumont et al., 2014). The fact that ribs, in contrast to long bones, do not have an isometric growth could also be an advantage for the growth record preservation. Due to the formation of the rib ridge, the medullary cavity seems to expand less on the posteromedial side during growth, resulting in lesser resorption of the primary bone tissue and therefore more recorded LAGs.

Institutional abbreviations – **ML**: Museu da Lourinhã, Lourinhã, Portugal; **SMA**: Sauriermuseum Aathal, Aathal, Canton Zürich, Switzerland.

2. Material

2.1. Sampled material

The following specimens used for this study represent a phylogenetical broad but incomplete selection of archosaurs including saurischians (Theropoda and Sauropoda), ornitischians (Stegosauria and Ornithopoda) and crocodylomorphs. All samples (excluding the literature data of sauropod SMA 0002) are from the Lusitanian Basin, western Portugal. All but one (*Baryonyx walkeri*) are dated from the Kimmeridgian–Tithonian Lourinhã Formation according to regional stratigraphic context, vertebrate fauna and strontium isotope dating (Mateus et al., 2014). This formation yields dinosaur bones, crocodylomorphs, pterosaurs, mammals, amphibians and other Jurassic vertebrates as well as teeth, eggs and tracks (e.g., Araújo et al., 2013; Hendrickx and Mateus, 2014; Milàn et al., 2005), providing a unique window into the terrestrial Late Jurassic fauna of Europe. This study includes dorsal rib histology from the proximal rib shaft of a *Camarasaurus* specimen used in Waskow and Sander (2014), as well as the following dorsal rib samples of specimens from the ML collections.

2.1.1. ML 433: Miragaia longicollum (Stegosauria)

Specimen ML 433 is the holotype of the dacentrurinae stegosaur *M. longicollum* (Mateus et al., 2009), from the Miragaia Member of the Lourinhã Formation, dated from the Kimmeridgian–Tithonian transition (about 152 M.a.) This specimen corresponds to a large individual up to 6.5 m long, with fused neurocentral sutures, and ossified tendons or cartilage located mainly in the ulna. The cervical portion is unusually long for stegosaurs due to the presence of 17 segments, and the most posterior cervical vertebrae being cervicalized dorsal elements (Mateus et al., 2009). Histology of *Miragaia* has never been studied except for the tail spines by Hayashi et al. (2008).

2.1.2. ML 439: Draconyx loureiroi (Ornithopoda)

Specimen ML 439 is the holotype of camptosaurid ornithopod *D. loureiroi* (Mateus and Antunes, 2001), from the Praia Azul Member of the Lourinhã Formation (Latest Kimmeridgian to earliest Tithonian), and is a poorly-known ankylopollexian, which is partly articulated but poorly preserved. The neurocentral suture fusion suggests that ML 439 is an adult, but tracks also suggest the occurrence of much larger individuals of ornithopod dinosaurs in the same region (Mateus and Milàn, 2008).

2.1.3. ML 370: Lourinhanosaurus antunesi (Theropoda; Avetheropoda)

Specimen ML 370 is the holotype of *L. antunesi* (Mateus, 1998), also from the Praia Azul Member of the Lourinhã Formation. It is a tetanuran theropod of uncertain affinity; recent phylogenetic analyses place *Lourinhanosaurus* as either a basal coelurosaurian (Carrano et al., 2012), a sinraptorid allosauroid (Benson et al., 2010) or a megalosaurid. The specimen appears to be an adult but no histological study has been done – bone histology has been documented on embryos only (de Ricqlès et al., 2001).

2.1.4. ML 1190: Baryonyx walkeri (Theropoda; Spinosauroidea)

Specimen ML 1190 is the theropod *B. walkeri* (Charig and Milner, 1986) found at Praia das Aguncheiras (Mateus et al., 2011). Stratigraphically, it belongs to the Papo Seco Formation (early Barremian) of Portugal. It is the only sample from the Early Cretaceous used in this analysis. The body size of this specimen is equivalent to that of the holotype of *B. walkeri* NHM R9951, which is identified as an adult (Charig and Milner, 1986), despite the fact that the neurocentral suture is often, but not always, open and unfused.

2.1.5. ML 426: Crocodylomorph (Crurotarsi)

Specimen ML 426 is a crocodylomorph collected in the late 1980s at Casal da Pedreira, in the vicinity of Lourinhã (Praia Azul Member, Lourinhã Formation, Kimmeridgian–Tithonian boundary). It preserves most of the axial skeleton, a few osteoderms, fragmentary limb elements but no skull. Taking into account the overall anatomy and size of these remains, this crocodylomorph may be a *Goniopholis* (Owen, 1841) but more study is needed. The vertebrae show fused but visible neurocentral sutures, suggesting the animal to be an adult.

2.2. Dorsal rib material described in the literature

SMA 0002: *Camarasaurus sp.* (Sauropoda): specimen SMA 0002 is one of the most complete and articulated *Camarasaurus* skeletons ever found. Its assignment to *Camarasaurus* based on several diagnostic features mentioned by Ikejiri (2004), McIntosh (2005), and Upchurch et al. (2004), but this attribution has been recently challenged by Mateus and Tschopp (2013), who identified it as *Cathetosaurus*, based on the morphology of the pelvic girdle and dorsal transverse processes. In more recent studies, however, it was again claimed to be a *Camarasaurus* specimen, based on its autopodial and preliminary unpublished phylogenetic analysis (Tschopp et al., 2015, 2016). The SMA 0002 specimen was found in the Upper Jurassic Morrison Formation (Kimmeridgian), which is situated in the central northern part of Wyoming, USA. It is the stratigraphically oldest *Camarasaurus* in the whole formation (Ayer, 2000; Waskow and Sander, 2014). With three-dimensional preservation, the small but mature individual lacks only the vomers, the splenial bones, the distal end of the tail, and one terminal phalanx of the right pes (Tschopp et al., 2015; Waskow and Sander, 2014). Former histological studies of the long bones and ribs suggest a senescent age of this individual (Klein and Sander, 2008; Waskow and Sander, 2014), with a growth record of 37 preserved LAGs (Waskow and Sander, 2014).

3. Methods

3.1. Thin sectioning

All samples were taken as complete cross-sections from well-preserved regions of the proximal rib shaft of the different taxa. First, molds of all sampled rib parts were made to enable the reconstruction of the missing bone slice after sampling. These molds were made with a two-component silicone “Provil novo” consisting of the base putty and its catalyst (proportion 1:1). Each rib was protected with a solution of Technovit 4071, a technical polymer. The two components of this polymer (powder and liquid) are usually used in a ratio of 2:1. Here we used a 3:1 ratio to make the liquid suspension more viscous to properly mold the whole sampling region of the rib shaft. The protected area then was cut with an automatic rock saw and cut into standard paleo-histological thin sections (see Chinsamy and Raath, 1992; Enlow and Brown, 1956; Lamm, 2007; Wells, 1989). After sawing, the hardened Technovit polymer was removed with acetone. Rib pieces were reconnected by putting the rib sections back in the mold and refilling the missing bone material with plaster. The authors decided to use whole cross-sections instead of core drilling (see Stein and Sander, 2009) to be sure that the most complete growth record preserved could be detected. Thin sections were analyzed under a Leica DML P polarizing microscope. The drawings of the sections were made with a Camera Lucida (Schott KL 1500 LCD). Photos were taken with a Leica DFC420 digital camera and processed with Imagic ImageAccess software.

3.2. Measurements for growth record evaluation

In some cases, the center of the medullary region, where the bone growth initiated, is not located in the center of the section itself. Thus, the center of the medullary region was determined following the method of Waskow and Sander (2014) by the intersection of the two imaginary lines connecting the two greatest diameters of the rib. Depending on the region of a section, the distance between two same LAGs vary laterally. We chose to measure the LAG interdistances in the thickest part of the cortex, on the posteromedial side of each section. The percentage of the preserved growth record was calculated by measuring the distance from the medullary region to the surface of the bone at the thickest part of the cortex, and the distance from the first visible LAG to the bone surface. By assuming that the first measured distance equals 100% of the growth record, preservation was calculated after the rule of proportion. Based on the assumption that the LAGs are generally more widely spaced in the inner part of the bone (Chinsamy-Turan, 2005), the distance between the center of the medullary region and the first visible LAG was measured and divided by the widest growth cycle to obtain the maximum number of resorbed LAGs.

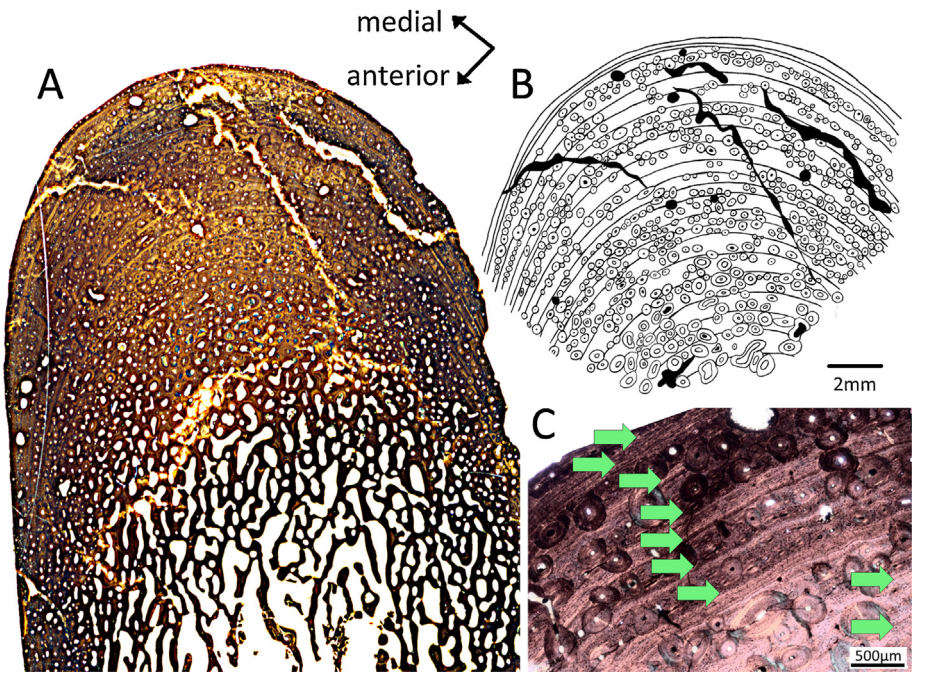

Fig. 1. Histological thin section of the posteromedial side of the dorsal rib of *Miragaia longicollum* (ML 433), which preserves the most complete growth record. A. Scanned image of the entire section. B. Drawing of the visible lines of arrested growth (LAGs) and the secondary osteons influencing the LAGs by destroying, or tracing them. C. Microscopic image of the section (PPL, cross-polarized, magnification?). All LAGs are marked with arrows.
Fig. 1. Section mince histologique du côté postéromédial de la côte dorsale de *Miragaia longicollum* (ML 433), qui préserve l'enregistrement le plus complet de la croissance. A. Image scan de la section entière. B. Dessin des *lines of arrested growth* (LAGs) visibles et des ostéones secondaires influençant les LAGs en les détruisant ou en les suivant. C. Image de la section au microscope (PPL, en polarisation croisée, agrandissement ?). Toutes les LAGS sont marquées par des flèches.

4. Results

4.1. Dorsal rib histological description

4.1.1. ML 433: M. longicollum (Stegosauria)

The well-preserved rib thin section shows a relatively large medullary region filled with spongiosa with reduced intertrabecular spaces in the middle. It is surrounded by a lamellar-zonal bone cortex greatly varying in thickness from 2 to 10 mm. Most primary bone tissue is preserved in the thickest part of the cortex building the rib ridge on the posteromedial side of the bone. The bone tissue is relatively poorly vascularized. The canals are predominantly oriented longitudinally. Only a few Sharpey's fibers oriented longitudinally, nearly parallel to the bones surface, are visible on the posterolateral side. Including the EFS, 22 annuli are counted, representing 68% of the growth record (Fig. 1). Most of them are preserved as clearly developed LAGs and only the innermost cycles are visible as polish lines (Sander, 2000). The outermost four LAGs, representing the EFS, are closely spaced (distances < 200 μm) with no significant primary bone tissue structures in between. The remodeling rate is relatively low with only about one-third of the primary bone tissue replaced by secondary osteons.

4.1.2. ML 439: D. loureiroi (Ornithopoda)

In contrast to *M. longicollum*, the well-preserved ribs of *D. loureiroi* only have a small medullary region completely filled with dense spongy bone tissue. As in the sample described before, the cortex thickness varies significantly around the section (5 mm to 18 mm). Again, most primary bone tissue is preserved in the posteromedial ridge of the rib (Fig. 2). Near the medullary cavity, fibrolamellar bone slowly changes into slower-growing lamellar-zonal bone towards the bones surface. Overall, the bone tissue is more vascularized than the section of *M. longicollum* described before, although the number of vascular canals (perforating the bone in all three directions) is still moderate. A higher amount of Sharpey's fibers is present with most of them, occurring again at the posterolateral side of the rib. Here, most fibers are oriented longitudinally, although the direction of the fibers changes around the section into several directions. Thirty growth cycles are counted. Similar to *M. longicollum*, the innermost growth cycles are only visible as polish lines. The outermost three LAGs comprise the EFS. Due to the small size of the medullary region, 86% of the growth record is preserved. There is nearly no cortical remodeling in the bone tissue. Only a few secondary osteons are visible, most of which are near the medullary cavity.

4.1.3. ML 370: L. antunesi (Theropoda; Avetheropoda)

In *L. antunesi*, the well-preserved histological section of the rib mainly consists of a large medullary cavity. The center of the medullary cavity is hollow, surrounded by a thick, spongy region. The thin cortex has a consistent thickness (2 mm) and consists of dense, highly vascularized primary bone tissue made of primary osteons. On the

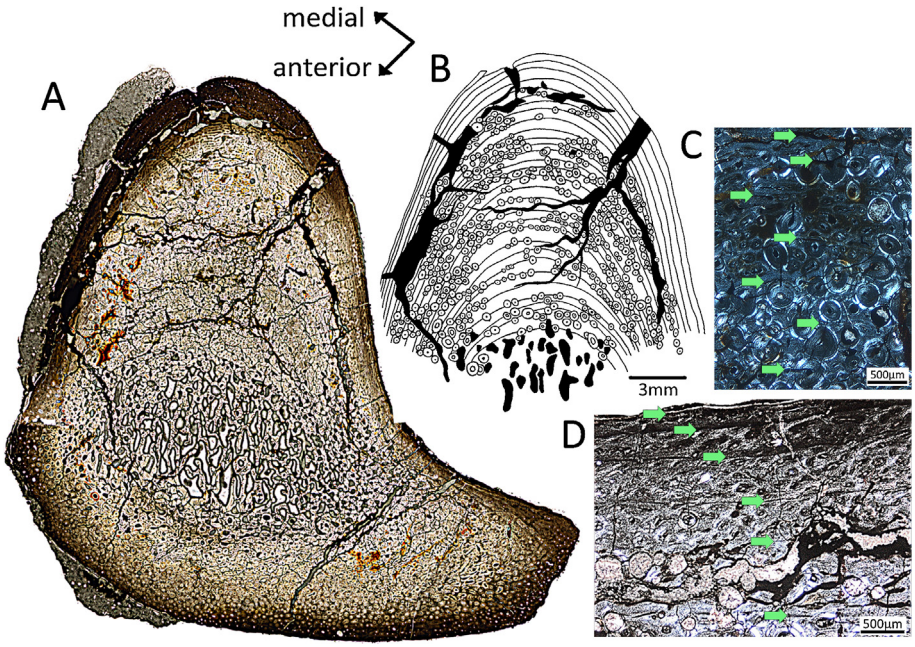

Fig. 2. Histological thin section of the posteromedial side of the dorsal rib of *Draconyx loureiroi* (ML 439), which preserves the most complete growth record. A. Macroscopic scan of the section. B. Drawing of the visible lines of arrested growth (LAGs) and the secondary osteons influencing the LAGs by destroying, or tracing them. C and D. Microscopic images of the section. All LAGs are marked with arrows.
Fig. 2. Section mince histologique du côté postéromédial de la côte dorsale de *Draconyx loureiroi* (ML 439), qui préserve l'enregistrement le plus complet de la croissance. A. Scan macroscopique de la section. B. Dessin des *lines of arrested growth* (LAGs) visibles et des ostéones secondaires influençant les LAGs en les détruisant ou en les suivant. C et D. Images de la section au microscope. Toutes les LAGs sont marquées par des flèches.

anteromedial and posterolateral side, most of the canals are oriented longitudinally and on the anterolateral and posteromedial side, some vascular canals are oriented radially. The tissue has a high osteocyte density and shows a vascularization similar to that of *D. loureiroii*, described before. A high amount of Sharpey's fibers is visible with most of the fibers oriented obliquely to the bone surface on the anterolateral and posteromedial side. On the opposite sides (anteromedial and posterolateral), Sharpey's fibers are oriented longitudinally. Due to the resorption of primary bone tissue caused by the expansion of the medullary cavity, only nine LAGs are preserved in the cortical bone area (Fig. 3). Nevertheless, these nine LAGs represent 57% of the growth record of the individual. There is no EFS visible, even if the last two LAGs seem to be more closely spaced than the others. No secondary osteons can be observed in this sample.

4.1.4. ML 1190: B. walkeri (Theropoda; Spinosauroidea)

All microanatomical patterns of *Baryonyx walker* are very similar to those of *D. loureiroii* described before. The relatively small medullary region is completely filled with cancellous bone. Cortex thickness again varies greatly (5 mm to 12 mm) around the section. Again, the primary bone tissue is well-preserved and moderately vascularized like in *D. loureiroii* and *L. antunesi*. Most vascular canals are oriented radially (especially on the posteromedial side) or longitudinally. Sharpey's fibers are visible and oriented obliquely or inclined to the surface. The 21 LAGs that have been counted represent 81% of the growth record (Fig. 4). The last seven LAGs comprise the EFS. Even if these LAGs seem to be more widely spaced than previously described, there are nearly no observable primary bone tissue structures in between each growth line. In contrast to *L. antunesi*, the number of secondary osteons is relatively high. About two thirds of the cortical bone is remodeled.

4.1.5. ML 426: Crocodylomorph (Crurotarsi)

The elongated medullary region is relatively small and completely filled with cancellous bone. The cortex shows the thickest area on both the posteromedial and anterolateral sides (cortex thickness varies from 1 mm to 4 mm). The well-preserved primary bone tissue consists of lamellar-zonal bone. It is extremely poorly vascularized. Only a few longitudinal canals are visible. Some Sharpey's fibers are visible, mainly on the posterolateral side. Here, their orientation is longitudinal. This orientation becomes more inclined towards the posteromedial and anterolateral sides. Posteromedially, 18 LAGs are preserved, representing 83% of the growth record (Fig. 5). An EFS is not preserved in this individual. Half of the original bone tissue is remodeled into Haversian bone.

5. Life history data evaluation

In the following section, life history parameters recorded during growth are summarized for every sampled taxon. By measuring the distances between the LAGs following the methods of Waskow and Sander (2014), a diagram has been created for each individual that shows the

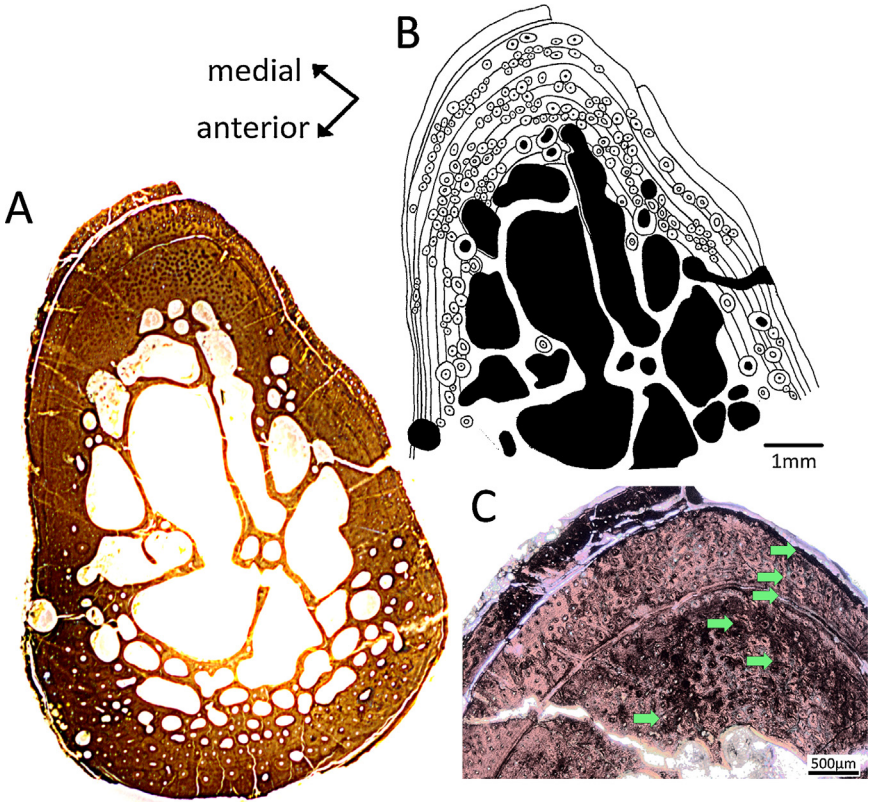

Fig. 3. Histological thin section of the posteromedial side of the dorsal rib of *Lourinhanosaurus antunesi* (ML 370), which preserves the most complete growth record. A. Macroscopic scan of the section. B. Drawing of the visible lines of arrested growth (LAGs) and the secondary osteons influencing the LAGs by destroying, or tracing them. C. Microscopic image of the section. All LAGs are marked with arrows.
Fig. 3. Section mince histologique du côté postéromédial de la côte dorsale de *Lourinhanosaurus antunesi* (ML 370), qui préserve l'enregistrement le plus complet de la croissance. A. Scan macroscopique de la section. B. Dessin des *lines of arrested growth* (LAGs) visibles et des ostéones secondaires influençant les LAGs en les détruisant ou en les suivant. C. Image de la section au microscope. Toutes les LAGs sont marquées par des flèches.

decrease in growth of the rib over somatic time (Figs. 6–10). Due to morphological changes during ontogeny (i.e. ribs are growing from proximal to distal; thus, the sampled proximal rib shaft of an adult represents the distal rib shaft when it was juvenile), these graphs are not accurate growth curves and cannot be used for mass estimations (Waskow and Sander, 2014), but they can be used to evaluate life history information. All general estimations requiring further explanations are discussed in the section following the discussion.

5.1. ML 433: M. longicollum (Stegosauria)

The primary bone tissue type and the low vascularization in this specimen suggest a relatively low deposition rate. The EFS indicates that the animal reached skeletal maturity before death. Using the method of retrocalculation, we can assume a maximum number of three to four missing growth cycles. Together with the 22 counted annuli, this would raise the age of skeletal maturity to about 25 years. If the EFS is excluded, the animal would have reached full size after 21 to 22 years of growth. Because of the relative completeness of the growth record preserved in the ribs, this is the most complete estimation for skeletal maturity in stegosaurs to date. Previous studies on this group have obtained a less complete growth record, or were only able to erect a general histologic ontogenetic stage (HOS) erected by Klein and Sander (2008) (Hayashi et al., 2009; Redelstorff and Sander, 2009; Redelstorff et al., 2013). Here, a significant decrease in growth is observed after the 11th counted LAG (Fig. 6). This is interpreted as the point of sexual maturity, which would be reached at 14 to 15 years old, that is, long before the animal was skeletally mature.

5.2. ML 439: D. loureiroi (Ornithopoda)

The preserved EFS indicates that the specimen must have been a fully grown individual. A retrocalculation suggests that a maximum number of 1-2 growth cycles are missing. Therefore, the animal reached its skeletal maturity after 27 to 31 years of growth, depending on whether the EFS is included or not. Like in the stegosaur *M. longicollum* (see above), a decrease in the rib growth rate is observed (Fig. 7), but it is not as prominent. Between the 11th and 16th counted LAG, this growth rate decrease is observed, and therefore, sexual maturity can be estimated to be reached between the ages of 12 and 17.

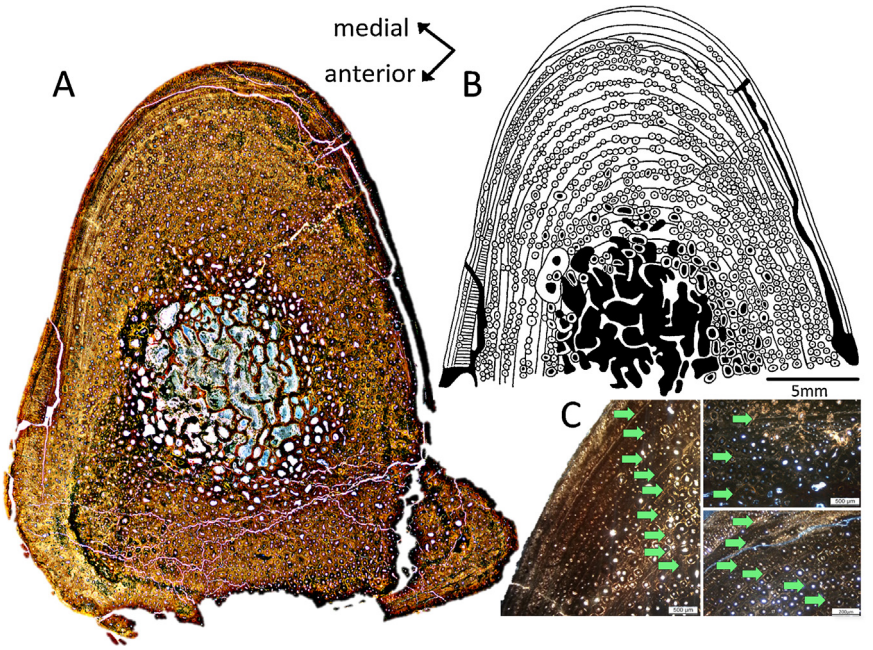

Fig. 4. Histological thin section of the posteromedial side of the dorsal rib of *Baryonyx walkeri* (ML 1190), which preserves the most complete growth record. A. Macroscopic scan of the section. B. Drawing of the visible lines of arrested growth (LAGs) and the secondary osteons influencing the LAGs by destroying, or tracing them. C. Microscopic images of the section. All LAGs are marked with arrows.
Fig. 4. Section mince histologique du côté postéromédial de la côte dorsale de *Baryonyx walkeri* (ML 1190), qui préserve l'enregistrement le plus complet de la croissance. A. Scan macroscopique de la section. B. Dessin des *lines of arrested growth* (LAGs) visibles et des ostéones secondaires influençant les LAGs en les détruisant ou en les suivant. C. Image de la section au microscope. Toutes les LAGs sont marquées par des flèches.

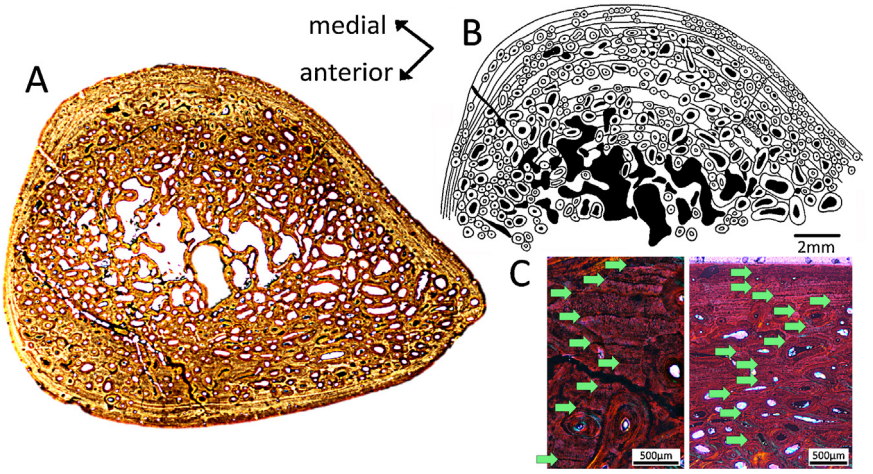

Fig. 5. Histological thin section of the posteromedial side of the dorsal rib of a crocodylomorph (ML 426), which preserves the most complete growth record. A. Macroscopic scan of the section. B. Drawing of the visible lines of arrested growth (LAGs) and the secondary osteons influencing the LAGs by destroying, or tracing them. C. Microscopic images of the section. All LAGs are marked with arrows.
Fig. 5. Section mince histologique du côté postéromédial de la côte dorsale d'un crocodylomorphe (ML 426), qui préserve l'enregistrement le plus complet de la croissance. A. Scan macroscopique de la section. B. Dessin des *lines of arrested growth* (LAGs) visibles et des ostéones secondaires influençant les LAGs en les détruisant ou en les suivant. C. Images au microscope de la section. Toutes les LAGs sont marquées par des flèches.

5.3. ML 370: L. antunesi (Theropoda; Avetheropoda)

Due to the expansion of the large medullary cavity of the specimen ML 370, only 57% of the growth record is preserved. Depending on the distance between LAGs used for retrocalculation, there are approximately five to eight LAGs missing in the inner cortex. An EFS is missing. The age at death of this skeletally immature individual is suggested to be between 14 and 17 years. Unfortunately, the LAGs counted in this section show up in different parts of the cortex. Some LAGs are only visible posteriorly, while others are only visible anteromedially. In contrast to all other sections, not all counted LAGs are visible in the thickest part of the cortex (the posteromedial side of the section), which means

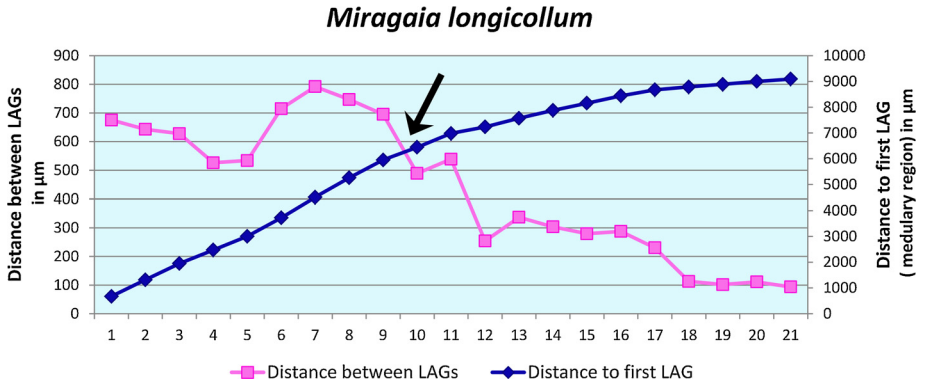

Fig. 6. Qualitative growth curve of *Miragaia longicollum* (ML 433) based on the lines of arrested growth (LAGs) counted in the dorsal rib, plotting cortical thickness increase with age (diamonds) and variation in cycle thickness with age (squares). The black arrow marks a decrease in growth, interpreted as the point of sexual maturity.
Fig. 6. Courbe de croissance qualitative de *Mirgaia longicollum* (ML 433) basée sur les *lines of arrested growth* (LAGs) dénombrées dans la côte dorsale, avec report de l'augmentation des épaisseurs corticales en fonction de l'âge (losanges) et de la variation d'épaisseur du cycle en fonction de l'âge (carrés). La flèche noire représente la diminution de croissance interprétée comme l'indication de la maturité sexuelle.

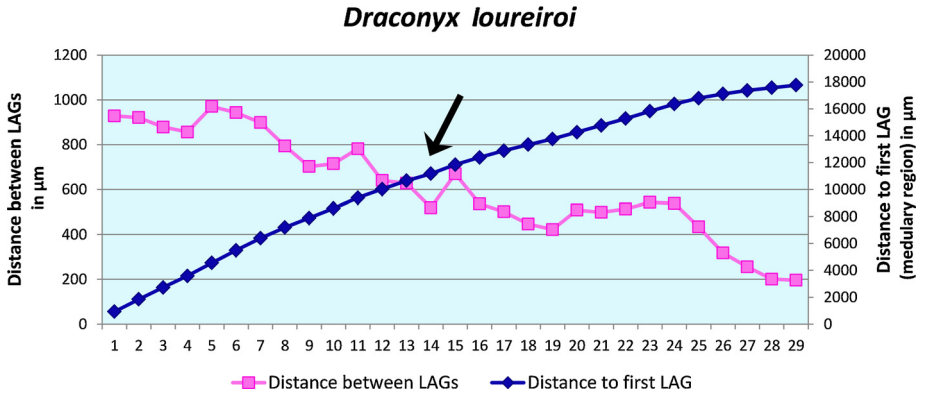

Fig. 7. Qualitative growth curve of *Draconyx loureiroi* (ML 439) based on the lines of arrested growth (LAGs) counted in the dorsal rib, plotting cortical thickness increase with age (diamonds) and variation in cycle thickness with age (squares). The black arrow marks a decrease in growth, interpreted as the point of sexual maturity.
Fig. 7. Courbe de croissance qualitative de *Dragonys loueiroi* (ML 439) basée sur les *lines of arrested growth* (LAGs) dénombrées dans la côte dorsale, avec report de l'augmentation de l'épaisseur corticale en fonction de l'âge (losanges) et de la variation d'épaisseur du cycle avec l'âge (carrés). La flèche noire représente la diminution de croissance interprétée comme l'indication de la maturité sexuelle.

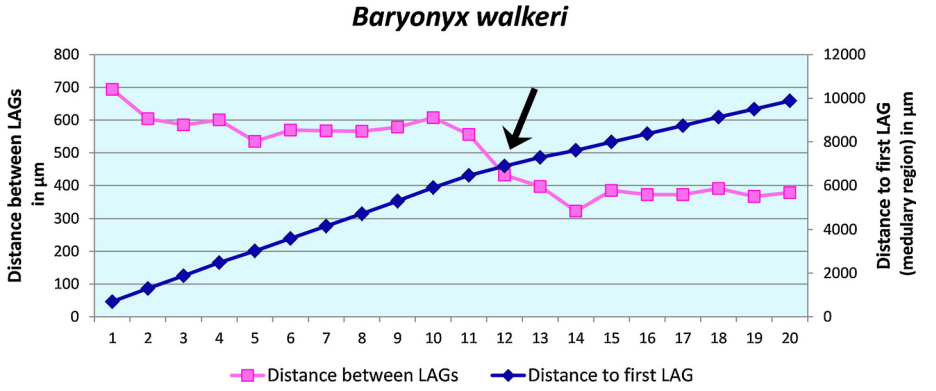

Fig. 8. Qualitative growth curve of *Baryonyx walkeri* (ML 1190) based on the lines of arrested growth (LAGs) counted in the dorsal rib, plotting cortical thickness increase with age (diamonds) and variation in cycle thickness with age (squares). The black arrow marks a decrease in growth, interpreted as the point of sexual maturity.
Fig. 8. Courbe de croissance qualitative de *Baryonyx walkeri* (ML 1190) basée sur les *lines of arrested growth* (LAGs) dénombrées dans la côte dorsale, avec report de l'augmentation de l'épaisseur corticale en fonction de l'âge (losanges) et variation d'épaisseur du cycle avec l'âge (carrés). La flèche noire représente la diminution de croissance, interprétée comme l'indication de la maturité sexuelle.

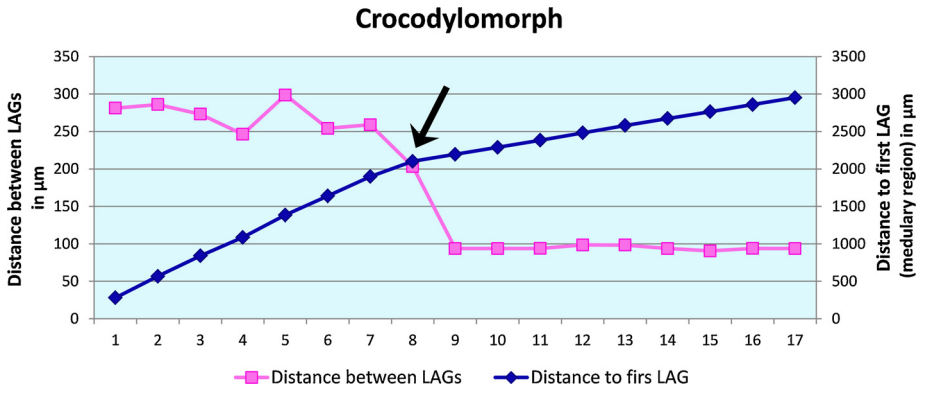

Fig. 9. Qualitative growth curve of a crocodylomorph (ML 426) based on the lines of arrested growth (LAGs) counted in the dorsal rib, plotting cortical thickness increase with age (diamonds) and variation in cycle thickness with age (squares). The black arrow marks a decrease in growth, interpreted as the point of sexual maturity.
Fig. 9. Courbe de croissance qualitative d'un crocodylomorphe (ML 426) basée sur les *lines of arrested growth* (LAGs) dénombrées dans la côte dorsale, avec report de l'augmentation de l'épaisseur corticale en fonction de l'âge (losanges) et variation d'épaisseur du cycle en fonction de l'âge (carrés). La flèche noire représente la diminution de croissance, interprétée comme l'indication de la maturité sexuelle.

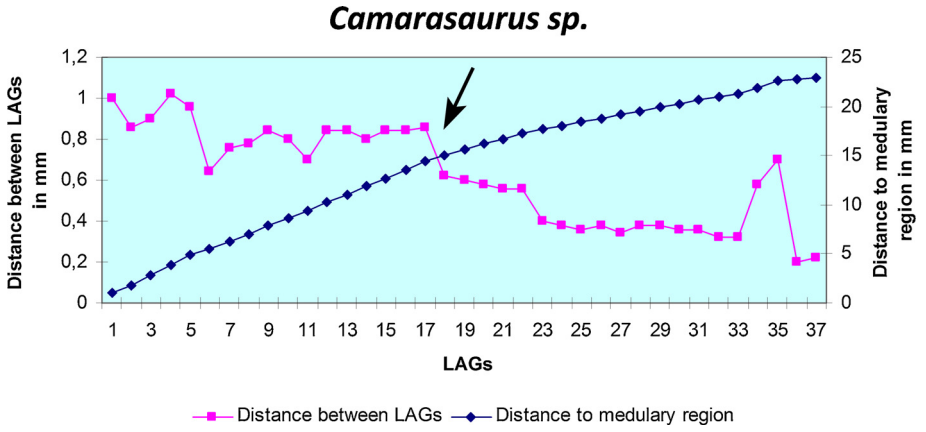

Fig. 10. Qualitative growth curve of *Camarasaurus* sp. (SMA 0002) based on the lines of arrested growth (LAGs) counted in the dorsal rib, plotting cortical thickness increase with age (diamonds) and variation in cycle thickness with age (squares). The black arrow marks a decrease in growth interpreted as the point of sexual maturity.
Fig. 10. Courbe de croissance qualitative de *Camara saurus* sp. (SMA 0002) basée sur les *lines of arrested growth* (LAGs) dénombrées dans la côte dorsale, avec report de l'augmentation de l'épaisseur corticale en fonction de l'âge (losanges) et variation d'épaisseur de cycle avec l'âge (carrés). La flèche noire représente la diminution de croissance interprétée comme l'indication de la maturité sexuelle.

that it was not possible to measure an accurate distance between the single LAGs to generate the growth graph. Therefore, no evidence for the point of sexual maturity is apparent.

5.4. ML 1190: B. walkeri (Theropoda; Spinosauroidea)

The specimen ML 1190 shows a clearly marked decrease in growth in the last 7 LAGs. Therefore, it is most likely that the individual was close to its maximum size. Including two to three missing LAGs computed by retrocalculation, it can be assumed that the animal died between the ages of 23 and 25 years, nearing its skeletal maturity. This is contrary to the anatomical evidence, that is, the neurocentral sutures are unfused, which suggests a rather earlier ontogenetic age. The occurrence of mature traits (based on the rib tissues) and subadult traits (partially unfused neurocentral sutures) could be interpreted as a possible paedomorphic trait for this taxon. Paedomorphosis has already been suggested in various aquatic or subaquatic tetrapods such as spinosaurids (Ibrahim et al., 2014), plesiosaurs (Araújo et al., 2015; Storrs, 1993) and temnospondyls (e.g., Steyer, 2000), and could be related to a swimming mode of locomotion. A more detailed analysis including a comparison of bone compactness using software such as Bone Profiler (e.g., Houssaye et al., 2016; Laurin et al., 2011; Steyer et al., 2004) would be useful for a more detailed lifestyle interpretation, but is beyond the scope of this study. A significant decrease in the growth rate after the 11th or 12th countable LAG suggests that the point of sexual maturity was reached at an age of 13 to 15 years (Fig. 8).

5.5. ML 426: Crocodylomorph (Crurotarsi)

The bone tissue shows a slow deposition rate. This specimen did not reach its skeletal maturity before its death. The

missing EFS indicates that the individual was indeed still growing. Considering one to two growth cycles are missing based on retrocalculation, the animal died at an age of 19 to 20 years. After the 9th counted LAG, a decrease in growth is observed (Fig. 9) and interpreted as the point of sexual maturity. In recent crocodiles and alligators, a significant sexual dimorphism has been observed (Chabreck and Joanen, 1979; Platt, 1996; Platt et al., 2008; Wilkinson and Rhodes, 1997). While the smaller females reach sexual maturity after nine to ten years, the larger males need about 20 years to reach the reproduction age. The estimated age of death together with the observed decrease in growth suggests that the small individual ML 426 most likely was a female that reached sexual maturity after 10 to 11 years.

6. Longevity and age determination based on the count of growth cycles in dorsal ribs

It has been shown that animals like crocodiles can live many years after reaching their skeletal maturity (e.g., Klein et al., 2009; Woodward et al., 2011b). Therefore, the number of counted LAGs for each studied individual cannot be equalized with longevity in all samples having an EFS. In contrast, if the animal did not reach its skeletal maturity before its death (which is documented by the absence of an EFS not attributed to preparation or pre-burial damage), its somatic age can be estimated by counting the LAGs and by taking into account the maximum number of LAGs missing due to remodeling or expansion of the medullary cavity. For all skeletally mature vertebrates, the estimated number of LAGs represents the time period they needed to reach full size (Castanet et al., 1993). The question whether the LAGs of the EFS should be included in the count of the LAGs is as controversial as the question of the annuality of the LAGs within the EFS (Horner et al., 1999). However, our diverse sample shows that the difference in the individual size is not significant if the EFS is excluded. By counting the LAGs excluding the EFS, the most reliable individual age before reaching skeletal maturity can be obtained.

7. General discussion

7.1. Viability of dorsal ribs for skeletochronology

While in the past ribs were studied very little, this study shows that dorsal ribs have a reliable growth record containing important information about life history traits. The reason to neglect dorsal ribs for histological studies until now may be because ribs have been historically claimed to be more strongly remodeled with secondary osteons than long bones (Enlow and Brown, 1958), given that even juvenile dinosaur individuals were initially claimed to show high amounts of Haversian bone (Nopcsa, 1933). Also, the strong histological variability within ribs has led to their exclusion from life history studies. In the comparative histology study by Horner et al. (2000), the ribs were found to be the worst skeletal elements for skeletochronology, showing the lowest LAGs count of all sampled bones. This can easily be explained by the fact that the authors sampled the wrong part of the rib. All of these reservations have been addressed by the study of Waskow and Sander (2014), who demonstrated that ribs in general have the most complete growth record at the proximal end of the rib shaft where growth initiated, and that (in contrast to the observations in long bones) the younger distal parts are more strongly remodeled than the older proximal ends. This current study further supports these findings. Even if only the proximal end of the rib shaft was sampled for each taxon, the rib histology observed confirms the findings of Waskow and Sander (2014). Furthermore, this study extends their observations to more taxa and different ontogenetic stages. Irrespective of the taxon, the rib position within the ribcage, the locomotion type, or the ontogenetic stage of the individual, all sampled taxa show a comparable growth record at this position in the rib. None of the samples were completely remodeled or lacked cyclicity. Even though this study validates ribs to be useful for histological studies, the major problem of varying bone apposition rates in ribs during ontogeny (also discussed in Waskow and Sander, 2014) still remains unresolved. Therefore, mass based growth curves based on the measurements between cycles of one individual is not reliable without calculating a correction formula. This work is currently in progress by Waskow and Griebeler (in prep.).

7.2. Comparability of the growth record preservation in ribs and long bones

Because ribs were not the focus of histological studies, one could argue that the growth record preserved in ribs might be different from that observed in well-studied long bones. However, Woodward et al. (2014) clearly showed that the growth record in different skeletal elements can be correlated using the example of an extant *A. mississippiensis*. All samples (even if not including dorsal ribs) show the same number of LAGs with the two closely spaced LAGs at the same relative position. Another more recent research paper by Wiersma et al. (2016) supports a good correlation between the growth record of ribs and long bones. The study of Waskow and Sander (2014) additionally shows that it is possible to correlate the growth record between ribs of a single individual independent of the extremely variable outer morphology.

Another point of criticism might be that there are no studies on modern animals verifying that ribs are equally good indicators for overall skeletal maturity as long bones. Because they are not weight-bearing bones, the possibility that their growth might stop earlier due to different restrictions compared to long bones cannot be excluded. However, even though ribs are not weight-bearing bones, to our knowledge, there is no significant allometric change during ontogeny between long bones and the rib cage in archosaurs. This justifies the assumption that these elements have no significant difference in their respective age at skeletal maturity. Additionally, the definition of skeletal maturity is the point where the animal's growth considerably slows down or stops. Histologically, this is reached at the beginning of an EFS. At this point, the lines of arrested growth are spaced significantly closer to each other without primary osteons, vascularization, etc. in between. For these reasons, these LAGs observed in the rib sections can be identified as the EFS, as it has been done before, for

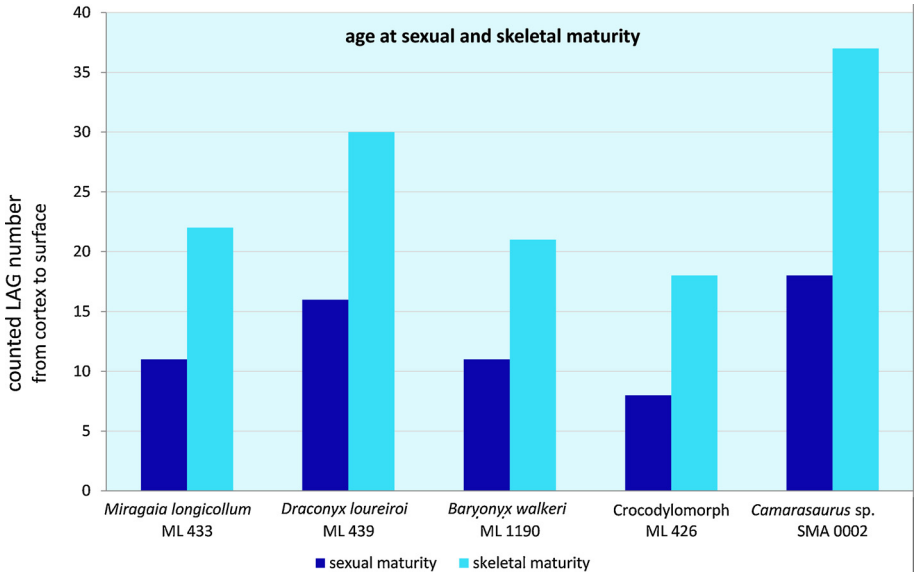

Fig. 11. Graph showing the number of counted growth cycles after which sexual and skeletal maturity were reached in the various taxa studied here.
Fig. 11. Graphique montrant le nombre de cycles de croissance décomptés, après lequel la maturité sexuelle et celle du squelette ont été atteintes dans les différents taxons étudiés ici.

example, by Erickson et al. (2004) and Waskow and Sander (2014). Due to the variation in distance between two given LAGs all around the cortex one could argue that the identification of an EFS is difficult. Nevertheless the EFS in ribs can be identified doubles and independent of the asymmetric deposition of bone material between the single LAGs, that is caused by morphological changes during ontogeny by looking at the area where the bone apposition rate is highest. If the distance between the LAGs here shows the conditions of an EFS its existence can be confirmed. Also, a comparison between the EFS in long bones and ribs of the same individual has been done (at least for sauropods) in the study of Waskow and Sander (2014) with all elements showing an EFS with the same number of LAGs. This additionally reinforces the assumption that skeletal maturity was reached simultaneously in ribs and long bones. However, the aim of this study is only to show the completeness of the growth record in different archosaur taxa to highlight the research potential of these undervalued skeletal elements. More comparative histological work on bone elements of the same individual, similar to the work of Werning and Nesbitt (2016), Wiersma et al. (2017), and Woodward et al. (2014), needs to be done for extinct archosaurs to underline the importance and comparability of ribs with limb bones.

7.3. *Implications for age at sexual maturity*

Sexual maturity is a major event in life history, and age estimation at sexual maturity in extinct animals is controversial (Chinsamy-Turan, 2005; Curry, 1999; Erickson, 2005; Erickson et al., 2007; Horner et al., 1999; Klein and Sander, 2007, 2008; Sander, 2000). For ecological reasons of survivorship, Dunham et al. (1989) theorized that large non-avian dinosaurs must have required 5 to 20 years to reach their sexual maturity. For sauropods, Sander (2000) argued that sexual maturity can be detected on the basis of a marked decrease in growth, well before the animal was fully grown. This significant decrease in growth corresponds to the inflection point of the growth curve (Griebeler et al., 2013). At this point, it is thought that the animal starts to allocate more resources for its reproduction, which are then no longer available for growth (Case, 1978a, 1978b; Sander, 2000). It is reasonable to assume that sexual maturity in non-avian theropods and ornithischians may occur well before full adult size (Erickson et al., 2007). This is coincident with the findings of Lee and Werning (2008), who reported on medullary bone (found only in breeding females) that occurs in specimens showing the same decrease in growth. This reduction of growth has been directly observed in large, recent reptiles such as turtles and crocodiles (Lance, 2003). In our sampled taxa from Portugal, as well as in the sauropod data point from the literature (Waskow and Sander, 2014), the inflection point mentioned above is reached at the halfway point of skeletal maturity (Figs. 10 and 11). We conclude that the decrease in growth rate marks the acquisition of sexual maturity in our study of a heterogeneous group of archosaur taxa including Ornithischia (stegosaurs and ornithopods) as well as Saurischia (theropods and sauropods) and crocodylomorphs.

8. Conclusions

Dorsal rib histology of all studied taxa shows a nearly complete growth record and is valuable for estimating individual age at skeletal maturity and, in some cases, age at death. Even with respect to morphological changes during ontogeny, the point of sexual maturity can also be estimated. In all the studied taxa showing a significant decrease in growth rate, sexual maturity is reached around halfway of skeletal maturity. However, the non-isometric growth of ribs impedes a growth curve calculation for

mass estimation. Therefore, this method cannot replace long bone examination for assessments of other information like maximum annual growth rate or metabolic rate. However, ribs do not typically resorb bone on the posteromedial side, preserving the first LAGs, which most likely are destroyed in long bones due to the expansion of the medullary cavity. As showed by this analysis and previous studies (e.g., D'Emic et al., 2015; Erickson et al., 2004; Houssaye and Bardet, 2012; Waskow and Sander, 2014), ribs record growth better than long bones, and are generally easier to sample. The fact that they are also generally more common in museum collections reinforces their crucial role in bone histology and skeletochronology.

Acknowledgments

We would like to thank Olaf Dülfer (University of Bonn, Bonn, Germany) for technical support and help during the process of thin sectioning, and Aurore Canoville, Jessica Mitchell, Janka Brinkkötter, and Moritz Eisele for their assistance with translation into French, English proofreading, and picture editing during manuscript preparation. We thank Carla Tomás for the skilled preparation of specimens and laboratory management. Many Thanks to the reviewers Armand de Ricqlès, Jean-Sébastien Steyer and Holly Woodward for their helpful reviews, and the editors, with special thanks to Michel Laurin and Jorge Cubo, for their editorial efforts and quick responses. Finally, we would like to thank the DFG for funding. This is contribution 170 of the DFG Research Unit 533 "Biology of the Sauropod Dinosaurs: The Evolution of Gigantism".

References

Altunişik, A., Ergül Kalayci, T., Gül, Ç., Özdemir, N., Tosunoğlu, M., 2014. A skeletochronological study of the smooth new *Lissotriton vulgaris* (Amphibia: Urodela) from an island and a mainland population in Turkey. It. J. Zool. 81 (3), 381–388.

Amprino, R., 1947. La structure du tissu osseux envisagée comme expression de différences dans la vitesse de l'accroissement. Arch. Biol. 58, 315–330.

Araújo, R., Castanhinha, R., Martins, R.M., Mateus, O., Hendrickx, C., Beckmann, F., Schell, N., Alves, L.C., 2013. Filling the gaps of dinosaur eggshell phylogeny: Late Jurassic Theropod clutch with embryos from Portugal. Sci. Rep. 3, 1924.

Araújo, R., Polcyn, M.J., Lindgren, J., Jacobs, L.L., Schulp, A.S., Mateus, O., Olímpio Gonçalves, A., Morais, M.L., 2015. New aristonectine elasmosaurid plesiosaur specimens from the Early Maastrichtian of Angola and comments on paedomorphism in plesiosaurs. Neth. J. Geosci. 94, 93–108, http://dx.doi.org/10.1017/njg.2014.43.

Ayer, J., 2000. The Howe Ranch Dinosaurs. Sauriermuseum Aathal, Zurich (95 p.).

Benson, R.B.J., Carrano, M.T., Brusatte, S.L., 2010. A new clade of archaic large-bodied predatory dinosaurs (Theropoda: Allosauroidea) that survived to the Latest Mesozoic. Naturwissenschaften 97 (1), 71–78.

Brochu, C.A., 1996. Closure of neurocentral sutures during crocodilian ontogeny: implications for maturity assessment in fossil archosaurs. J. Vert. Paleontol. 16, 49–62.

de Buffrénil, V., de Ricqlès, A., Ray, C.E., Domning, D.P., 1990. Bone histology of the ribs of the archaeocetes (Mammalia: Cetacea). J. Vert. Paleontol. 10 (4), 455–466.

Caetano, M.H., 1990. Use and results of skeletochronology in some urodeles *Triturus marmoratus*, Latreille 1800 and *Triturus boscai*, Lataste 1879. Ann. Sci. Nat. Zool. 11, 197–199.

Canoville, A., Buffrénil, V., Laurin, M., 2016. Microanatomical diversity of amniote ribs: an exploratory quantitative study. Biol. J. Linn. Soc. 118 (4), 706–733, http://dx.doi.org/10.1111/bij.12779.

Carrano, M.T., Benson, R.B.J., Sampson, S.D., 2012. The phylogeny of Tetanurae (Dinosauria: Theropoda). J. Syst. Palaeontol. 10.2 (2012), 211–300.

Case, T.J., 1978a. On the evolution and adaptive significance of postnatal growth rates in the terrestrial vertebrates. Quart. Rev. Biol. 53, 243–282.

Case, T.J., 1978b. Speculations on the growth rate and reproduction of some dinosaurs. Paleobiology 4, 320–328.

Castanet, J., 1994. Age existimation and longevity in reptiles. Gerontology 40, 174–192.

Castanet, J., Smirina, E., 1990. Introduction to the skeletochronological method in amphibians and reptiles. Ann. Sci. Nat. Zool. (Paris) II, 191–197.

Castanet, J., Francillon-Vieillot, H., Meunier, F.J., de Ricqlès, A., 1993. Bone and individual aging. In: Hall, B.K. (Ed.), Bone. Volume 7: Bone Growth—B. CRC Press, Boca Raton, FL, USA, pp. 245–283.

Castanet, J., Grandin, A., Abourachid, A., de Ricqlès, A., 1996. Expression of growth dynamic in the structure of the periosteal bone in the mallard, *Anas platyrhynchos*. C. R. Acad. Sci. Paris, Ser. III 319, 301–308.

Castanet, J., Croci, S., Aujard, F., Perret, M., Cubo, J., de Margerie, E., 2004. Lines of arrested growth in bone and age estimation in a small primate: *Microcebus murinus*. J. Zool. 2631, 31–39.

Chabreck, R.H., Joanen, T., 1979. Growth rates of American alligators in Louisiana. Herpetologica, 51–57.

Charig, A.J., Milner, A.C., 1986. *Baryonyx*, a remarkable new theropod dinosaur. Nature 324 (6095), 359–361.

Chinsamy, A., Raath, M.A., 1992. Preparation of bone for histological study. Palaentol. Afr. 29, 39–44.

Chinsamy, A., Hillenius, W.J., 2004. Physiology of non-avian dinosaurs. In: Weishampel, D.B., Dodson, P., Osmólska, H. (Eds.), The Dinosauria, second ed. University of California Press, Berkeley, CA, USA, pp. 643–659.

Chinsamy-Turan, A., 2005. The Microstructure of Dinosaur Bone. Deciphering Biology with Fine-Scale Techniques. The John Hopkins University Press, Baltimore, MD, USA (195 p.).

Currey, J.D., 2002. Bones. Structure and Mechanics. Princeton University Press, Princeton, NJ, USA (436 p.).

Curry, K.A., 1999. Ontogenetic histology of *Apatosaurus* (Dinosauria:Sauropoda): new insights on growth rates and longevity. J. Vert Paleontol. 19, 654–665.

D'Emic, M.D., Smith, K.M., Ansley, Z.T., 2015. Unusual histology and morphology of the ribs of mosasaurs (Squamata). Palaeontology 58 (3), 511–520.

Dumont, M., Borbely, A., Kaysser-Pyzalla, A., Sander, P.M., 2014. Long bone cortices in a growth series of *Apatosaurus* sp. (Dinosauria: Diplodocidae): geometry, body mass, and crystallite orientation of giant animals. Biol. J. Linn. Soc. 112 (4), 782–798.

Dunham, A.E., Overall, K.L., Porter, W.P., Forster, C.A., 1989. Implications of ecological energetics and biophysical and developmental constraints for life history variation in dinosaurs. In: Farlow, J.O. (Ed.), Paleobiology of the Dinosaurs. Geological Society of America Special Paper 238, Boulder, CO, USA, pp. 1–19.

Enlow, D.H., Brown, S.O., 1956. A comparative histological study of fossil and recent bone tissue. Part. I. Texas J. Sci. 8, 405–443.

Enlow, D.H., Brown, S.O., 1957. A comparative histological study of fossil and recent bone tissues. Part II. Texas J. Sci. 9 (2), 186–204.

Enlow, D.H., Brown, S.O., 1958. A comparative histological study of fossil and recent bone tissues. Part III. Texas J. Sci. 10 (2), 187–230.

Erickson, G.M., Makovicky, P.J., Currie, M.A., Norell, S.A., Yerby, C.A., Brochu, C.A., 2004. Gigantism and comparative life history parameters of tyrannosaurid dinosaurs. Nature 430, 772–775.

Erickson, G.M., 2005. Assessing dinosaur growth patterns: a microscopic revolution. Trends Ecol. Evol. 20, 677–684.

Erickson, G.M., de Ricqlès, A., de Buffrénil, V., Molnar, R.E., Bayless, M.K., 2003. Vermiform bones and the evolution of gigantism in Megalania—how a reptilian fox became a lion. J. Vert. Paleontol. 23 (4), 966–970.

Erickson, G.M., Rogers, K.C., Varricchio, D.J., Norell, M.A., Xu, X., 2007. Growth patterns in brooding dinosaurs reveals the timing of sexual maturity in non-avian dinosaurs and genesis of the avian condition. Biol. Lett. 3, 558–561.

Fronimos, J.A., Wilson, J.A., 2017. Neurocentral suture complexity and stress distribution in the vertebral column of a sauropod dinosaur. Ameghiniana 54 (1), 36–49, http://dx.doi.org/10.5710/AMGH.05.09.2016.3009.

Garcia, B.J., 2011. Skeletochronology Of The American Alligator (Alligator Mississippiensis): Examination Of The Utility Of Elements For Histological Study (Master Thesis).

Griebeler, E.M., Klein, N., Sander, P.M., 2013. Aging, maturation and growth of Sauropodomorph dinosaurs as deduced from growth curves using long bone histological data: an assessment of methodological constraints and solutions. PLoS One 8 (6), e67012, http://dx.doi.org/10.1371/journal.pone.0067012.

Hall, B.K., 2005. Bone and Cartilage: Developmental and Evolutionary Skeletal Biology. Elsevier Academic Press, London (787 p.).

Hayashi, S., Carpenter, K., Watabe, M., Mateus, O., Barsbold, R., 2008. Defensive weapons of thyreophoran dinosaurs: histological comparisons and structural differences in spikes and clubs of ankylosaurs and stegosaurs. J. Vert. Paleontol. 28 (Supplement to 3), 89A–90A.

Hayashi, S., Carpenter, K., Suzuki, D., 2009. Different growth patterns between the skeleton and osteoderms of *Stegosaurus* (Ornithischia: Thyreophora). J. Vert. Paleontol. 29 (1), 123–131.

Hayashi, S., Houssaye, A., Nakajima, Y., Chiba, K., Ando, T., Sawamura, H., Inuzuka, N., Kaneko, N., Osaki, T., 2013. Bone inner structure suggests increasing aquatic adaptations in Desmostylia (Mammalia, Afrotheria). PLoS One 8 (4), e59146, http://dx.doi.org/10.1371/journal.pone.0059146.

Hendrickx, C., Mateus, O., 2014. Abelisauridae (Dinosauria: Theropoda) from the Late Jurassic of Portugal and dentition-based phylogeny as a contribution for the identification of isolated theropod teeth. Zootaxa 3759, 1–74.

Horner, J., de Ricqlès, A., Padian, K., 1999. Variation in dinosaur skeletochronology indicators: implications for age assessment and physiology. Paleobiology 25, 295–304.

Horner, J.R., de Ricqlès, A., Padian, K., 2000. Long bone histology of the hadrosaurid dinosaur *Maiasaura peeblesorum*: growth dynamics and physiology based on an ontogenetic series of skeletal elements. J. Vert. Paleontol. 20 (1), 115–129 (doi: 10.1671/0272-4634(2000)020[0115:LBHOTH]2.0.CO;2).

Houssaye, A., 2009. "Pachyostosis" in aquatic amniotes: a review. Integr. Zool. 4 (4), 325–340.

Houssaye, A., 2013. Bone histology of aquatic reptiles: what does it tell us about secondary adaptation to an aquatic life? Biol. J. Linn. Soc. 108 (1), 3–21.

Houssaye, A., Bardet, N., 2012. Rib and vertebral microanatomical characteristics of hydropelvic mosasauroids. Lethaia 45 (2), 200–209.

Houssaye, A., Waskow, K., Hayashi, S., Cornette, R., Lee, A.H., Hutchinson, J.R., 2016. Biomechanical evolution of solid bones in large animals: a microanatomical investigation. Biol. J. Linnean Soc. 117, 350–371, http://dx.doi.org/10.1111/bij.12660.

Hutton, J.M., 1986. Age determination of living Nile crocodiles from the cortical stratification of bone. Copeia 1986, 332–341.

Ibrahim, N., Sereno, P.C., Dal Sasso, C., Maganuco, S., Fabbri, M., Martill, D.M., Iurino, D.A., 2014. Semiaquatic adaptations in a giant predatory dinosaur. Science 345 (6204), 1613–1616.

Ikejiri, T., 2004. Anatomy of *Camarasaurus lentus* (Dinosauria: Sauropoda) from the Morrison Formation (Late Jurassic), Thermopolis, central Wyoming, with PALAEOELECTRONICA.ORG59 determination and interpretation of ontogenetic, sexual dimorphic, and individual variation in the genus. Fort Hays State University, Kansas, UMI (Unpublished Masters Thesis).

Ikejiri, T., 2012. Histology-based morphology of the neurocentral synchondrosis in *Alligator mississippiensis* (Archosauria, Crocodylia). Anat. Rec. (Hoboken) 295 (1), 18–31.

Irmis, R.B., 2007. Axial skeleton ontogeny in the Parasuchia (Archosauria: Pseudosuchia) and its implications for ontogenetic determination in archosaurs. J. Vert. Paleontol. 27, 350–361.

Klein, N., Sander, P.M., 2007. Bone histology and growth of the prosauropod dinosaur *Plateosaurus engelhardti* von Meyer, 1837 from the Norian bone beds of Trossingen (Germany) and Frick (Switzerland). Spec. Pap. Palaeontol. 77, 169–206.

Klein, N., Sander, P.M., 2008. Ontogenetic stages in the long bone histology of sauropod dinosaurs. Paleobiology 34, 247–263.

Klein, N., Scheyer, T., Tütken, T., 2009. Skeletochronology and isotopic analysis of an individual specimen of *Alligator mississippiensis* Daudin, 1802. Fossil Rec. 12, 121–131.

Klein, N., Christian, A., Sander, P.M., 2012. Histology shows that elongated neck ribs in sauropod dinosaurs are ossified tendons. Biol. Lett. 8 (6), 1032–1035.

Köhler, M., Marín-Moratalla, N., Jordana, X., Aanes, R., 2012. Seasonal bone growth and physiology in endotherms shed light on dinosaur physiology. Nature 487, 358–361.

Lamm, E.T., 2007. Paleohistology widens the field of view in paleontology. Microsc. Microanal. 13 (S02, Supplement), 50–51.

Lance, V.A., 2003. Alligator physiology and life history: the importance of temperature. Exp. Gerontol. 38, 801–805.

Laurin, M., Meunier, F.J., Germain, D., Lemoine, M., 2007. A microanatomical and histological study of the paired fin skeleton of the Devonian sarcopterygian *Eusthenopteron foordi*. J. Paleontol. 81 (1), 143–153.

Laurin, M., Canoville, A., Germain, D., 2011. Bone microanatomy and lifestyle: a descriptive approach. C. R. Palevol 10, 381–402.

Lee, A.H., Werning, S., 2008. Sexual maturity in growing dinosaurs does not fit reptilian growth models. Proc. Natl. Acad. Sci. USA 105, 582–587.

McIntosh, J.S., 2005. The genus *Barosaurus* Marsh (Sauropoda, Diplodocidae). In: Tidwell, V., Carpenter, K. (Eds.), Thunder-lizards: the Sauropodomorph Dinosaurs. Indiana University Press, Bloomington, IN, USA, pp. 38–777.

de Margerie, E., Robin, J.-P., Verrier, D., Cubo, J., Groscolas, R., Castanet, J., 2004. Assessing a relationship between bone microstructure and growth rate: a fluorescent labelling study in the king penguin chick (*Aptenodytes patagonicus*). J. Exp. Biol. 207, 869–879.

Mateus, O., 1998. *Lourinhanosaurus antunesi*, a new Upper Jurassic allosauroid (Dinosauria: Theropoda) from Lourinhã, Portugal. Mem. Acad. Cien. Lisboa 37, 111–124.

Mateus, O., Tschopp, E., 2013. *Cathetosaurus* as a valid sauropod genus and comparisons with *Camarasaurus*. J. Vert. Paleontol., Program and Abstracts 2013, 173.

Mateus, O., Antunes, M.T., 2001. *Draconyx loureiroi*, a new camptosauridae (Dinosauria, Ornithopoda) from the Late Jurassic of Lourinhã, Portugal. Ann. Paleontol. 87 (1), 61–73.

Mateus, O., Milàn, J., 2008. Ichnological evidence for giant ornithopod dinosaurs in the Upper Jurassic Lourinha Formation, Portugal. Oryctos 8, 47–52.

Mateus, O., Maidment, S.C., Christiansen, N.A., 2009. A new long-necked 'sauropod-mimic' stegosaur and the evolution of the plated dinosaurs. Proc. Roy. Soc. B: Biol. Sci. 276 (1663), 1815–1821.

Mateus, O., Dinis, J., Cunha, P.P., 2014. Upper Jurassic to Lowermost Cretaceous of the Lusitanian Basin, Portugal – landscapes where dinosaurs walked. Cien. Terra Special issue No. VIII, 1–37.

Mateus, O., Araújo, R., Natário, C., Castanhinha, R., 2011. A new specimen of the theropod dinosaur *Baryonyx* from the Early Cretaceous of Portugal and taxonomic validity of Suchosaurus. Zootaxa 2827, 54–68.

Milàn, J., Christiansen, P., Mateus, O., 2005. A three-dimensionally preserved sauropod manus impression from the Upper Jurassic of Portugal: Implications for sauropod manus shape and locomotor mechanics. Kaupia 14, 47–51.

Nopcsa, F.B., 1933. On the histology of the ribs in immature and half-grown trachodont dinosaurs. Proc. Zool. Soc. London 103 (1), 221–226, http://dx.doi.org/10.1111/j.1096-3642.1933.tb01588.x.

Owen, R., 1841. Report on British fossil reptiles. Rep. Br. Assoc. Adv. Sci. 11, 60–204.

Padian, K., Horner, J.R., 2004. Dinosaur physiology. In: Weishampel, D.B., Dodson, P., Osmólska, H. (Eds.), The Dinosauria, second ed. University of California Press, Berkeley, CA, USA, pp. 660–671.

Pancharatna, K., Kumbar, S.M., 2013. Bone growth marks in tropical wall lizard, *Hemidactylus brooki*. Russ. J. Herpetol. 12 (2), 107–110.

Platt, S.G., (Unpublished PhD Thesis) 1996. The Ecology and Status Morelet's Crocodile in Belize. Clemson University, SC, USA.

Platt, S.G., Rainwater, T.R., Thorbjarnarson, J.B., McMurry, S.T., 2008. Reproductive dynamics of a tropical freshwater crocodilian: Morelet's crocodile in northern Belize. J. Zool. 275 (2), 177–189.

Redelstorff, R., Sander, P.M., 2009. Long and girdle bone histology of *Stegosaurus*: implications for growth and life history. J. Vert. Paleontol. 29 (4), 1087–1099.

Redelstorff, R., Hübner, T.R., Chinsamy, A., Sander, P.M., 2013. Bone histology of the Stegosaur *Kentrosaurus aethiopicus* (Ornithischia: Thyreophora) from the Upper Jurassic of Tanzania. Anat. Rec. (Hoboken) 296 (6), 933–952.

de Ricqlès, A., 1975. Recherches paléohistologiques sur les os longs des tétrapodes VII. — Sur la classification, la signification fonctionnelle et l'histoire des tissus osseux des tétrapodes. Première partie, structures. Ann. Paleontol. 61, 51–129.

de Ricqlès, A., 1976. On bone histology of fossil and living reptiles with comments on its functional and evolutionary significance. In: Bellairs, A.D.A., Cox, C.B. (Eds.), Linnean Society Symposium Series 3. Linnean Society, London, pp. 123–150.

de Ricqlès, A., 1983. Cyclical growth in the long limb bones of a sauropod dinosaur. Acta Palaeontol. Pol. 28, 225–232.

de Ricqlès, A., Meunier, F.J., Castanet, L., Francillon-Vieillot, H., 1991. Comparative microstructure of bone. In: Hall, B.K. (Ed.), Bone. CRC Press, Boca Raton, FL, USA, pp. 1–78.

de Ricqlès, A., Mateus, O., Antunes, M.T., Taquet, P., 2001. Histomorphogenesis of embryos of Upper Jurassic theropods from Lourinhã (Portugal). C. R. Acad. Sci. Paris, Ser. IIa 332, 647–656.

de Ricqlès, A., Padian, K., Knoll, F., Horner, J.R., 2008. On the origin of high growth rates in archosaurs and their ancient relatives: complementary histological studies on Triassic archosauriforms and the problem of a "phylogenetic signal" in bone histology. Ann. Paleontol. 94 (2), 57–76.

Sander, P.M., 2000. Long bone histology of the Tendaguru sauropods: implications for growth and biology. Paleobiology 26, 466–488.

Sander, P.M., Klein, N., Stein, K., Wings, O., 2011. Sauropod bone histology and its implications for sauropod biology. In: Klein, N., Remes, K., Gee, C.T., Sander, P.M. (Eds.), Biology of the Sauropod Dinosaurs: Understanding the Life of Giants. Indiana University Press, Bloomington, IN, USA, pp. 276–302.

Sander, P.M., Klein, N., Buffetaut, E., Cuny, G., Suteethorn, V., Le Loeuff, J., 2004. Adaptive radiation in sauropod dinosaurs: bone histology indicates rapid evolution of giant body size through acceleration. Org. Divers. Evol. 4 (3), 165–173.

Smirina, E.M., Tsellarius, A.Y.T., 1996. Aging, longevity and growth of the desert monitor lizard (*Varanus griseus* Daud.). Russ. J. Herpetol. 3, 130–142.

Smirina, E.M., Ananjeva, N.B., 2007. Growth layers in bones and acrodont teeth of the agamid lizard *Laudakia stoliczkana* (Blanford, 1875) (Agamidae, Sauria). Amphibia–Reptilia 28 (2), 193–204.

Snover, M.L., Balazs, G.H., Murakawa, S.K., Hargrove, S.K., Rice, M.R., Seitz, W.A., 2013. Age and growth rates of Hawaiian hawksbill turtles (*Eretmochelys imbricata*) using skeletochronology. Mar. Biol. 160 (1), 37–46.

Stein, K., Sander, P.M., 2009. Histological core drilling: a less destructive method for studying bone histology. In: Brown, M.A., Kane, J.F., Parker, W.G. (Eds.), Methods in Fossil Preparation: Proc. First Annual Fossil Preparation and Collections Symposium, Petrified Forest National Park, 2008. University of Nebraska State Museum Holbrook, Arizona, pp. 69–80.

Steyer, J.S., 2000. Ontogeny and phylogeny in temnospondyls: a new method of analysis. Zool. J. Linn. Soc. 130, 449–467.

Steyer, J.S., Laurin, M., Castanet, J., de Ricqlès, A., 2004. First histological and skeletochronological data on temnospondyl growth: palaeoecological and palaeoclimatological implications. Palaeogeogr., Palaeoclimatol., Palaeoecol. 206 (3), 193–201.

Storrs, G.W., 1993. Function and phylogeny in sauropterygian (Diapsida) evolution. Am. J. Sci. 293A, 63–90.

Tschopp, E., Wings, O., Frauenfelder, T., Brinkmann, W., 2015. Articulated bone sets of manus and pedes of *Camarasaurus* (Sauropoda, Dinosauria). Palaeontol. Electron. 18 (2), 1–65.

Tschopp, E., Wings, O., Frauenfelder, T., Rothschild, B.M., 2016. Pathological phalanges in a camarasaurid sauropod dinosaur and implications on behaviour. Acta Palaeontol. Pol. 61 (1), 125–134.

Turvey, S.P., Green, O.R., Holdaway, R.N., 2005. Cortical growth marks reveal extended juvenile development in New Zealand moa. Nature 435, 940–943.

Upchurch, P., Barrett, P.M., Dodson, P., 2004. Sauropoda. In: Weishampel, D.B., Dodson, P., Osmólska, H. (Eds.), The Dinosauria, second ed. University of California Press, Berkeley and Los Angeles, California, pp. 259–322.

Waskow, K., Sander, P.M., 2014. Growth record and histological variation in the dorsal ribs of *Camarasaurus* sp. (Sauropoda). J. Vert. Paleontol. 34 (4), 852–869.

Wells, N.A., 1989. Making thin sections. In: Feldmann, R.M., Chapman, R.E., Hannibal, J.T. (Eds.), Paleotechniques. Department of Geological Sciences, University of Tennessee, Knoxville, Tennessee, pp. 120–129.

Werning, S., Nesbitt, S.J., 2016. Bone histology and growth in Stenaulorhynchus stockleyi (Archosauromorpha: Rhynchosauria) from the Middle Triassic of the Ruhuhu Basin of Tanzania. C. R. Palevol 15, 169–181.

Wiersma, K., Canoville, A., Siber, H.-J., Sander, P.M., 2017. Testing hypothesis of skeletal unity using bone histology: the case of the sauropod remains from the Howe-Stephens and Howe Scott quarries (Morrison Formation, Wyoming). Palaeontol. Electron. (submitted).

Wilkinson, P.M., Rhodes, W.E., 1997. Growth rates of American alligators in coastal South Carolina. J. Wildlife Manage. 61, 397–402.

Woodward, H.N., Rich, T.H., Chinsamy, A., Vickers-Rich, P., 2011a. Growth dynamics of Australia's polar dinosaurs. PLoS One 6 (8), e23339, http://dx.doi.org/10.1371/journal.pone.0023339.

Woodward, H.N., Horner, J.R., Farlow, J.O., 2011b. Osteohistological evidence for determinate growth in the American alligator. J. Herpetol. 45 (3), 339–342.

Woodward, H.N., Horner, J.R., Farlow, J.O., 2014. Quantification of intraskeletal histovariability in *Alligator mississippiensis* and implications for vertebrate osteohistology. Peer J 2, e422.